Stereoelectronic Effects in N−C−S and N−N−C Systems: Experimental and *ab Initio* AIM Study

Ivan S. Bushmarinov,[†] Mikhail Yu. Antipin,[†] Vnira R. Akhmetova,[‡] Guzel R. Nadyrgulova,[‡] and Konstantin A. Lyssenko*,[†]

A. N. Nesmeyanov Institute of Organoelement Compounds, Russian Academy of Sciences, 119991, Vavilov Str., 28, Moscow, Russia, and Institute of Petrochemistry and Catalysis, Russian Academy of Sciences, 141 Prospekt Oktyabrya, 450075 Ufa, Russian Federation

Received: January 15, 2008; Revised Manuscript Received: February 26, 2008

The energy of stereoelectronic interactions in N−C−S and N−N−C systems in tetrahydro[1,3,4]thiadiazolo[3,4-*c*][1,3,4]thiadiazole was estimated by means of R. W. Bader's quantum theory of "atoms in molecules" (AIM) and natural bond orbital analysis (NBO). The results were compared with those obtained by analysis of $\rho(r)$ derived from high-resolution X-ray diffraction data. The analysis of the data obtained allowed one to find a correlation between geometric characteristics of the stereoelectronic interactions, NBO mixing energies and the AIM properties of atoms. Significant variations of nitrogen atom atomic basin populations in different conformers were explained by sterical interactions between their electron lone pairs.

Introduction

The generalized anomeric effect is one of the fundamental concepts commonly used for prediction of the most energetically favored conformation in various classes of compounds. Indeed, both experimental and theoretical data show that in the R−X−C−Y systems, where X is bearing a lone pair and Y is more electronegative than the carbon atom, the *gauche* conformation is generally the most stable.[1–4] The first theoretical model described the anomeric effect in terms of dipole−dipole interaction,[1] and it was considered to be destabilizing due to electrostatic repulsion of electron pairs.[2] The different interpretation, which is now widely accepted, explains the anomeric effect in terms of charge transfer from X's lone pairs (hereinafter *lp*) to the σ^*_{C-Y} antibonding orbital. In this model, called also the stereoelectronic model (SM), the anomeric effect is described as a special case of general stereoelectronic effects, which are summarized in books by Kirby[3] and Deslongchamps.[4]

Further investigations have revealed that the anomeric effect does not always define conformational preferences that in certain cases may be explained by repulsion of lone pairs and steric effects, as the stereoelectronic effects do not significantly affect the system's energy.[5,6] In particular, the analysis of chemical bonding in terms of the natural bond orbital (NBO) scheme[7] has demonstrated that in some systems hyperconjugative interactions like charge transfer from X's lone pairs to antibonding orbitals on nonpolar bonds compensate the anomeric effect to large extent, and thus should be taken into account.[8,9]

Some other methods, like Fourier analysis of the potential energy curve for conformer transformation proposed by Radom and co-workers,[10] were used for quantitative estimation of anomeric effect.[5,6] It has been shown recently that examination of the latter within the quantum theory of atoms in molecules (AIM)[11] provides significant supplement to NBO analysis. It recovers the anomeric effect by changes in energies and electron populations obtained by integration of corresponding functions over atomic basins.[12,13] These results were achieved on O−C−O and N−C−N systems, but it has been demonstrated before that the C−S bond is polar enough for anomeric interaction to occur,[8] thus the N−C−S system should display the same trends.

To compare the influence of various stereoelectronic interactions on the topological parameters such as atomic energy and charge, we performed an investigation of tetrahydro[1,3,4]thiadiazolo[3,4-*c*][1,3,4]thiadiazole (**1**). Depending on the conformers *lp*-N−N−C, *lp*-N−C−S, *lp*-N−C−H, *lp*-S−C−N and *lp*-S−C−H stereoelectronic interactions may be expected. The potential presence of five different types of stereoelectronic interactions is of particular interest for estimation of general trends in AIM properties of atoms involved. As the total electron density function $\rho(r)$ can be obtained from XRD,[14,15] one can expect that anomeric effects can be evaluated on the basis of the experimental data using the AIM methods. Indeed, it is well-known that usage of experimental $\rho(r)$ function makes it possible to evaluate such parameters as potential energy density[16a,b] and even to estimate the crystal lattice energy.[18a–d] Thus it was intriguing to check the applicability of this approach for analysis of stereoelectronic interactions in **1** basing on differences in atomic energy values, which are expected to be rather small, according to ref 13.

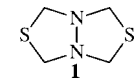

1

Experimental Part and Computational Details

Crystals of **1** ($C_4H_8N_2S_2$, M = 148.24) are monoclinic, space group *C*2/*c*, at 100 K: a = 12.1589(19), b = 4.7880(8), c = 10.7556(15) Å; β = 102.048(7)°; V = 612.36(16) Å^3; Z = 4 (Z' = 0.5); d_{calc} = 1.608 g cm^{-3}; μ(Mo Kα) = 0.754 cm^{-1}; F(000) = 312. Intensities of 15064 reflections were measured with a Bruker SMART APEX2 CCD diffractometer [λ(Mo Kα) = 0.71073Å, ω-scans, 2θ < 105°] and 3568 independent

* Corresponding author. E-mail: kostya@xrlab.ineos.ac.ru.
† A. N. Nesmeyanov Institute of Organoelement Compounds. E-mail: nk@anrb.ru.
‡ Institute of Petrochemistry and Catalysis.

10.1021/jp800384k CCC: $40.75
Published on Web 05/08/2008

reflections [$R_{int} = 0.0237$] were used in further refinement. The structure was solved by direct methods and refined by the full-matrix least-squares technique against F^2 in the anisotropic-isotropic approximation. Hydrogen atoms were located from the Fourier synthesis of the electron density and refined in the isotropic approximation. The refinement converged to w$R2$ = 0.0571 and GOF = 1.000 for all independent reflections ($R1$ = 0.0196 was calculated against F for 3025 observed reflections with $I > 2\sigma(I)$). All calculations were performed using SHELXTL-Plus 5.0.[19]

The multipole refinement was carried out within the Hansen−Coppens formalism[20] using the XD program package.[21,22] Before the refinement, C−H bond distances were normalized to the values obtained from the neutron data.[23] The refinement was carried out against F and converged to $R = 0.0153$, Rw = 0.0143 and GOF = 0.9645 for 3067 merged reflections with $I > 3\sigma(I)$ and $F_{obs} > 0.9$. The total electron density function was positive everywhere and the maxima of residual electron density located in the vicinity of sulfur nuclei were not more than 0.252 e Å^{-3}. Topological analysis of the experimental $\rho(r)$ function was carried out using the WinXPRO program package.[24]

The estimation of the kinetic energy [$g(r)$] was based on the Kirzhnits approximation[25] relating it with values of the $\rho(r)$ and its derivatives: $g(r) = (3/10)(3\pi^2)^{2/3}[\rho(r)]^{5/3} + (1/72)|\nabla\rho(r)|^2/\rho(r) + (1/6)\nabla^2\rho(r)]$.

The usage of this relationship in conjunction with the virial theorem $(2g(r) + v(r) = (1/4)\nabla^2\rho(r))$[11] provided the value of potential energy density [$v(r)$] in the CPs from experimental diffraction data. Moreover, this method allows one to estimate the atomic energy by integration of electron energy density function $h_e(r) = g(r) + v(r)$ over the atomic basin (see, for example, refs 26 and 27).

Ab initio calculations of the isolated molecule **1** were performed with the Gaussian98 program package[28] at the MP2 and B3LYP levels. Preliminary search and optimization of all conformers of **1** were performed by molecular mechanics methods within MM3 force field.[29] Full optimization for each conformer was carried out with the 6-311G* (B3LYP) and 6-311G** (MP2) basis sets. As convergence criteria, the extremely tight threshold limits of 2×10^{-6} and 6×10^{-6} au were applied for the maximum force and displacement. To enhance DFT calculation accuracy and increase the reliability of low frequency mode, the pruned (99590) grid (keyword Grid=Ultrafine) has been used. The optimization at DFT level of theory was followed by the evaluation of the harmonic vibration frequencies. Topological analysis of the $\rho(r)$ function[30] and integration over the atomic basins[31] using the MORPHY98 program package[30] was based on the charge density functions obtained by MP2 and B3LYP calculations.

The charge leakage for studied conformers did not exceed 0.015 e. Despite the small values of Lagrangian integrated over atomic surfaces (up to 0.003 au), the energy of molecule obtained by the summation of atomic contribution was systematically lower than MP2 energy. Taking into account that the above difference in each case was merely the same (0.3 ± 0.01 au), we can be aware that the atomic energies do not contain systematic errors.

Results

In the crystal molecule **1** occupies a special position on a C_2 axis passing through the middle of the N(1)−N(1A) bond (Figure 1). Its five-membered cycles had twist conformations with both carbon atoms deviating from S−N−N planes by 0.63 Å. Analysis of the C−S and C−N bond lengths (Table S1−S2)

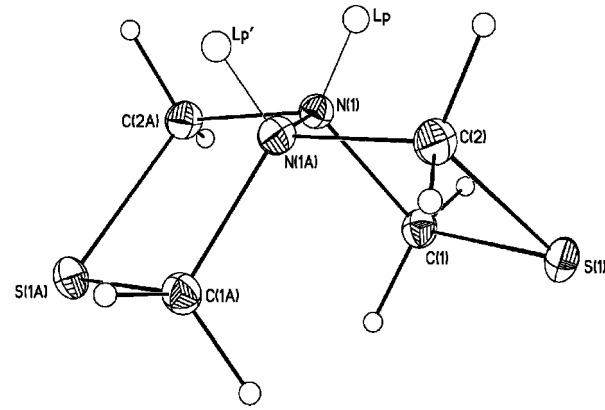

Figure 1. The general view of **1** in representation of atoms by thermal ellipsoids (p = 50%). The hypothetical positions of electron lone pairs are designated as Lp and Lp′.

has demonstrated that the C(2)−N(1A) bond is considerably shorter (by 0.0458(8) Å) than the equivalent C(1)−N(1) bond, and the C(2)−S(1) bond is longer than C(1)−S(1) by 0.0462(8) Å. These differences could not be explained by intermolecular interactions. Analysis of crystal packing revealed only the presence of weak S···C and S···H contacts of 3.49 and 2.97 Å, which is only slightly smaller than the sum of van der Waals radii[32] of corresponding atoms. Thus, the examination of bond lengths indicated the occurrence of pronounced *lp*-N(1A)−C(2)−S(1) stereoelectronic interactions. This suggestion was confirmed by the value of *lp*-N(1A)−C(2)−S(1) pseudotorsion angle, equal to 159°, being rather favorable for such type of interaction. Hereinafter the position of nitrogen's lone pair was estimated in the assumption of Gillespie's valence shell electron pair repulsion theory (VSEPR).[33] But the *lp*-N(1A)−N(1)−C(1) pseudotorsion angle of 171° calculated in the same assumptions shows that from the geometrical point of view the *lp*-N(1A)−N(1)−C(1) interaction is even more favorable. Moreover, some *lp*-N−C−H dihedral angles allow us to expect the corresponding *lp*-N−C−H stereoelectronic interactions (Table 2S). Thus, the geometric characteristics do not provide unambiguous information on the nature and contribution of stereoelectronic interactions in the compound studied.

More precisely, the conclusions about the disposition of lone pairs with respect to chemical bonds in **1** can be drawn from the analysis of static deformational electronic density (DED) and electron localization function (ELF) maps in the S(1)−C(2)−N(1A) plane (Figure 2). As can be seen from the former, an electron density accumulation attributed to the nitrogen's lone pair is antiperiplanar to the S(1)−C(2) bond and adjacent to depletion of DED. For calculations of the ELF function from experimental data, Tsirelson's approach[34] has been used in which the kinetic energy density is estimated by means of Kirznits approximation.[25] The accuracy of this method for analysis of the electron lone pair domains from XRD data has been proved in a number of investigations.[34,35]

It is noteworthy that the ELF function is more physically supported and does not suffer from the choice of reference function as the DED one does, especially in the case of a bifurcation analysis developed by Savin et al.[36] The examination is performed by clipping the values of ELF function less than a given value f. This operation produces attractors of ELF function called f-domains. At very low f values (less than 0.5) there is only one f-domain covering the entire molecular system, which divides to smaller domains with the increase of f. At high values there are only unseparable (irreducible) f-domains left.

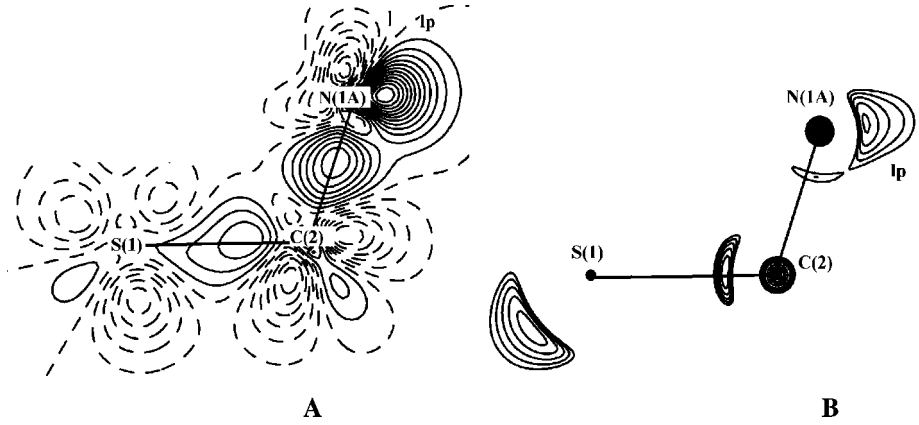

Figure 2. Experimental DED (A) and ELF (B) distribution in the S(1)C(2)N(1A) plane. Contours are drawn with 0.05 e Å^{-3} step for (A) and 0.02 for (B). The negative values for DED map are shown by dashed lines, for ELF the values above $f = 0.80$ are shown.

TABLE 1: Bond Lengths and Some Topological Parameters Obtained from Experimental Data and at Different Computational Levels for 1[a]

	X-ray diffraction data			B3LYP/6-311G*			MP2/6-311G**		
bond	d, Å	$\rho(r)$, e Å^{-3}	ε	d, Å	$\rho(r)$, e Å^{-3}	ε	d, Å	$\rho(r)$, e Å^{-3}	ε
C(1)−S(1)	1.8142(4)	1.05	0.13	1.835	1.17	0.11	1.815	1.22	0.11
C(2)−S(1)	1.8605(4)	1.03	0.14	1.894	1.04	0.12	1.860	1.11	0.12
C(1)−N(1)	1.4891(4)	1.68	0.07	1.494	1.70	0.07	1.488	1.72	0.05
N(1A)−C(2)	1.4435(4)	1.78	0.08	1.432	1.91	0.05	1.440	1.88	0.05
N(1)−N(1A)	1.4411(5)	1.96	0.12	1.428	2.09	0.10	1.429	2.09	0.09
C(1)−H(1A)	1.080*	0.27	0.04	1.095	0.28	0.02	1.097	0.28	0.01
C(1)−H(1E)	1.080*	0.27	0.04	1.089	0.28	0.02	1.091	0.28	0.01
C(2)−H(2E)	1.080*	0.27	0.03	1.088	0.28	0.02	1.091	0.28	0.01
C(2)−H(2A)	1.080*	0.27	0.03	1.087	0.28	0.02	1.089	0.28	0.02

[a] The ideal value of 1.080 Å was assumed for C−H bonds basing on neutron data.

The surface of an f-domain is called a basin and the basins of irreducible f-domains have a clear chemical interpretation: the basins containing a nucleus (except a proton) are called core basins and correspond to atoms, and other basins are called valence basins and represent bonds and lone pairs. The map of ELF function with value >0.8 in the S(1)−C(2)−N(1A) plane (Figure 2B) displays the expected core attractors for S(1), C(2) and N(1A) as well as valence attractors corresponding to the C−N and C−S bonds and sulfur and nitrogen lone pairs, confirming the conclusions made from the values of pseudotorsion angles and DED map.

The critical point (CP) search in the crystal of **1** has revealed the presence of CP (3, −1) for all expected chemical bonds and two CP (3, +1) for five-membered cycles. The topological properties in the CP (3, −1), namely the values of $\rho(r)$, ε and potential energy density [$v(r)$] were distinct for different C−N and C−S bonds, and this correlates with the corresponding difference in the bond lengths (Table 1). Two (3, +1) critical points attributed to the formation of five-membered rings were also located.

In addition to intramolecular bonds, a number of intermolecular S···H, S···S, N···H and H···H contacts were observed. They were found to be rather weak and correspond to the closed-shell interactions. In particular, the values of $\rho(r)$ in their CP's (3, −1) vary in the range 0.03−0.05 e Å^{-3} and the energies of contacts estimated within Espinosa's correlation scheme[17] are in the range 0.7−1.1 kcal/mol (see Table S3). The summation of the latter using the procedure described in[18a] leads to lattice energy value equal to 14.9 kcal/mol, which is rather reasonable for the molecule with such functional groups (see ref 37).

For more details on total electron density in the compound studied, the interatomic surfaces for all atoms were determined and electronic population, energy and Lagrangian of the $\rho(r)$ were integrated over the atomic basins (Ω). The results of integration for non-hydrogen atoms are represented in Table 2.

According to these values, the C(1) atom, being not involved in the N−C−S anomeric interaction, is characterized by larger electron population and significantly lower electron energy than C(2) one. But the energy difference between these atoms cannot be chosen as describing the *lp*-N(1A)−C(2)−S(1) stereoelectronic interaction, as C(1) could also be involved in additional *lp*-N(1A)−N(1)−C(1) interaction. Moreover, the atomic energies of carbons could also be affected by N−C−H and S−C−H stereoelectronic interactions, which cannot be estimated from X-ray diffraction data.

To check the validity of the experimental data and evaluate the energy of stereoelectronic interactions quantitatively, all stable conformers of the compound **1** (Figure 3) were located and further optimized at the B3LYP/6-311G(d) and MP2/6-311G(d,p) levels. The harmonic vibrational frequencies were also calculated for all conformers at the B3LYP level to characterize optimized stationary points (Table 3). All conformers were analyzed by NBO at B3LYP computational level.

Conformer **1**, as it is observed in crystal, has C_2 symmetry and twist−twist conformation of cycles. With the only exception of some shortening of the N−N bond by ca. 0.01 Å, all geometric parameters in the isolated state are almost equal to experimental ones in the crystal. This conformer appeared to be the global minimum of energy for the system studied. The NBO data (see Table S4) confirmed the presence of strong *lp*-N(1A)−C(2)−S(1) (12.1 kcal/mol) and *lp*-N(1A)−N(1)−C(1) (7.4 kcal/mol) stereoelectronic interactions.

In the conformer **1B** the bi-cycle is characterized by the twist−twist conformation with nitrogen's lone pairs arranged

TABLE 2: Comparison of Integral Properties of Atomic Basins ($E(\Omega)$, au; $N(\Omega)$, e; and $L(\Omega) \times 10^3$, au) for Conformer 1 Obtained at Different Computational Levels and with Experimental Data Derived from XRD[a]

	XRD			B3LYP/6-311G*			MP2/6-311G**		
	$N(\Omega)$	$E(\Omega)$	$L(\Omega) \times 10^3$	$N(\Omega)$	$E(\Omega)$	$L(\Omega) \times 10^3$	$N(\Omega)$	$E(\Omega)$	$L(\Omega) \times 10^3$
S(1)	15.96	−399.8223	0.03	16.06	−398.5152	1.16	16.00	−397.8373	1.05
N(1)	7.59	−54.8508	0.29	7.62	−54.9772	1.78	7.64	−54.9360	−1.02
C(1)	5.83	−38.0435	−0.27	5.85	−37.8802	−2.56	5.83	−37.8250	−0.17
C(2)	5.79	−38.0011	−0.54	5.74	−37.8209	−1.57	5.72	−37.7574	0.43
H(1A)	0.95	−0.6228	−0.20	0.94	−0.6023	0.21	0.97	−0.6168	0.19
H(1E)	0.98	−0.6329	−0.20	0.93	−0.6000	0.39	0.95	−0.6084	0.38
H(2E)	0.95	−0.6009	0.02	0.93	−0.5956	0.35	0.95	−0.6086	0.35
H(2A)	0.94	−0.6069	−0.11	0.92	−0.5969	0.41	0.94	−0.6072	0.41

[a] The convenient atomic charge can be obtained by subtracting the value of electronic population from the atomic number.

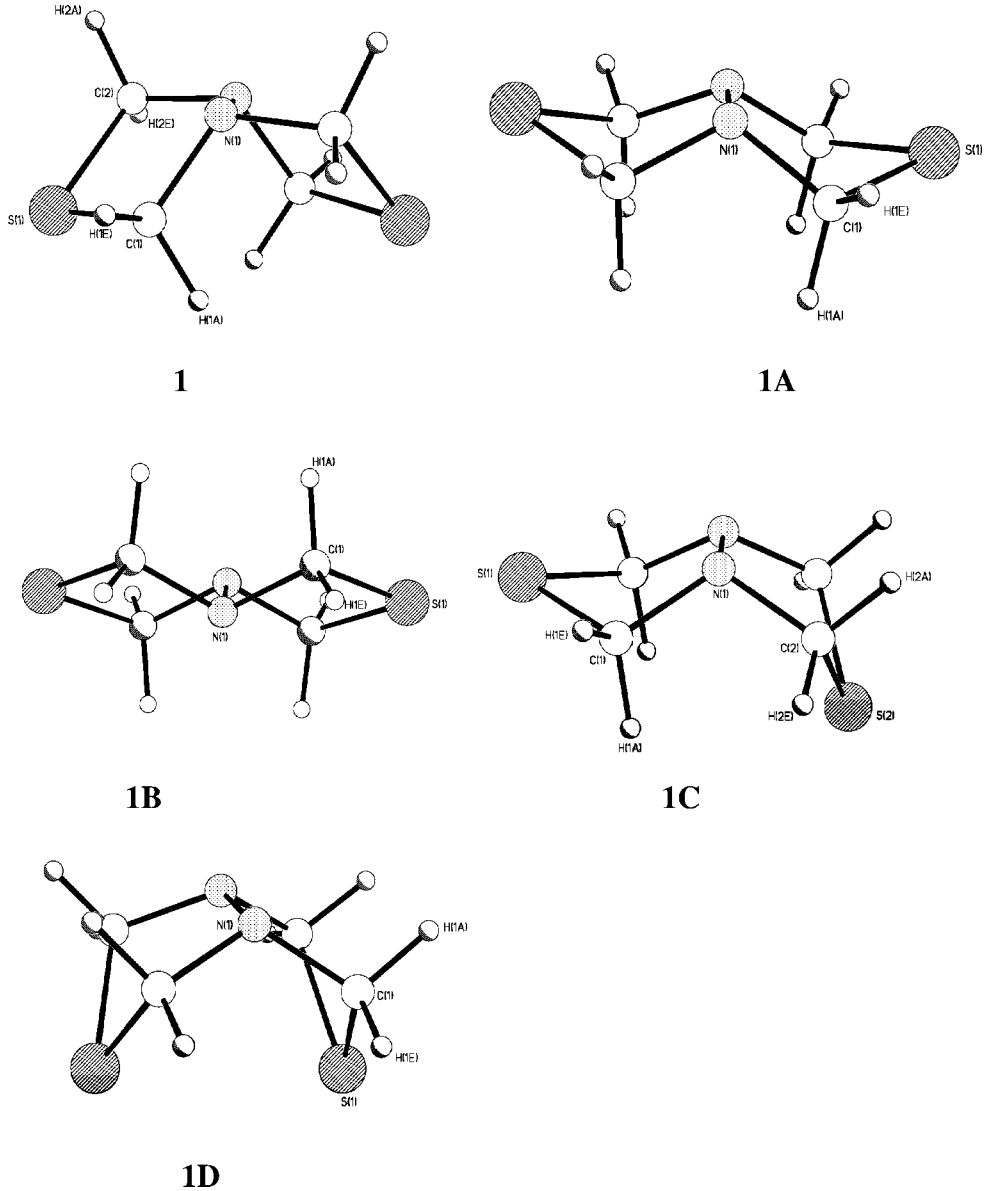

Figure 3. General view of the conformers of **1**. Labels are given only for symmetry independent atoms. Axial hydrogens are denoted by letter A and equatorial by letter E.

antiperiplanar, excluding any possibility of *lp*-N−N-*lp* interaction (Figure 3). The inversion of one nitrogen atom, as compared to conformer **1**, and thus exchange of the symmetry point group to C_{2h} led to equalizing of C−S and C−N bonds (1.825 and 1.458 Å), lengthening of the N−N bond (1.471 Å) and changes in C−H bond lengths. The antiperiplanar arrangement of nitrogen's lone pair to the C(1)–H(1A) bond and lengthening of this bond to 1.099 Å (0.003 Å longer than the longest C−H bond in conformer **1**) allowed us to suppose that N−C−H anomeric interactions in this conformer are more pronounced. The NBO analysis (Table S5) confirms this suggestion, indicating relatively strong *lp*-N−C−H (4.7 kcal/mol) and *lp*-S−C−H (5.9 kcal/mol) stereoelectronic interactions, weak *lp*-S−C−N (2.6 kcal/mol) and no other $n_N \rightarrow \sigma^*_{N-C}$ charge transfers.

TABLE 3: Relative Stability of Conformers of 1 According to B3LYP and MP2 Calculations

	B3LYP	ZPE (B3LYP)[a]	delta (kcal/mol)[b]	MP2 energy	delta (kcal/mol)[b]	symmetry point group
1	−1063.173337	0.12756 (0)	0.00	−1061.296644	0.00	C_2
1A	−1063.149523	0.12572 (1)	13.79	−1061.270929	14.98	C_{2v}
1B	−1063.161985	0.12709 (0)	6.83	−1061.284483	7.33	C_{2h}
1C	−1063.161109	0.12683 (0)	7.22	−1061.283378	7.87	C_s
1D	−1063.16312	0.12693 (1)	6.01	−1061.268077	17.53	C_{2v}

[a] The number of imaginary frequencies is given in parentheses. [b] Delta were calculated by taking ZPE into account.

The conformer **1C** has the envelope−envelope conformation of bi-cyclic system with the sulfur atoms deviating by 0.92 and 0.93 Å from the plane of the rest atoms (Figure 3). The molecule has C_s symmetry, and sulfur atoms are unequivalent; i.e., the S(2) atom could possibly be involved in N−C−S anomeric interactions, and the S(1) atom cannot (*lp*-N−C−S dihedral angles are 87.8 and 152.4°, respectively). Indeed, according to NBO data (Table S6) the *lp*-N(1)−C(2)−S(2) interaction is rather strong (10.4 kcal/mol), but it is weaker than the *lp*-N(1A)−C(2)−S(1) (12.1 kcal/mol) one in conformer **1**. Additionally, NBO revealed in this conformer the presence of rather weak *lp*-N−N−C (<2 kcal) interactions.

Conformers **1A** and **1D**, being local energy maxima with low-frequency imaginary frequencies, both have envelope−envelope conformations (Figure 3). The geometrical characteristics of conformers allowed us to expect the presence of strong *lp*-N−C−S stereoelectronic interactions in conformer **1D** and their absence in **1A.** The NBO analysis for conformer **1D** proved that $n_N \rightarrow \sigma^*_{C-S}$ charge transfer is characterized by rather high energy (9.28 kcal/mol).

To examine the bonding pattern in the conformers, the AIM analysis of $\rho(r)$ has been performed. The critical point search has revealed that for all conformers with the only exception for **1D** the characteristic set of CPs is identical to corresponding one in the crystal. In contrast, the occurrence of a shortened intramolecular S···S contact (3.223 Å) in **1D** leads to the presence of additional BCP attributed to S···S bonding interactions and consequently to formation of two ring CP (3, +1) and one cage CP (3, +3). The value of $\rho(r)$ in the CP (3, −1) is equal to 0.06 e Å^{-3}, which is close to corresponding values for similar intramolecular contacts (see, for example, ref 38). The energy of the S···S interaction estimated within Espinosa's correlation scheme is equal to 1.7 kcal/mol. It should be noted that with the exception of Laplacian values, all parameters in CP (3, −1) in the crystalline and isolated states are close to each other and the difference between MP2 and B3LYP data is comparable with the difference between DFT and experimental data. Furthermore, the integral properties of atomic basins ($N(\Omega)$ and $E(\Omega)$) for conformer **1** followed the same trends as it was experimentally observed.

A similar tendency was found for the differences in the $N(\Omega)$ and $E(\Omega)$ values for C(1) and C(2) atoms at both B3LYP and MP2 levels (Table 2). It should be noted that such qualitative agreement is not so evident *a priori*, but it was recently observed and discussed in detail by Matta et al.[39] At the same time, the integral values for hydrogen atoms obtained within MP2 calculations led to better results. In particular, the values of $N(\Omega)$ as well as $E(\Omega)$ correlated with the C−H bond lengths with correlation coefficients (hereinafter CC) exceeding 95%. At the same time, the CC values for $\rho(r)$ obtained at the B3LYP level are considerably lower. The rather small values of $L(\Omega)$ obtained for hydrogen atoms (see Table 2) allow us to discuss even small changes in atomic energy of hydrogens, see, for example, ref 40. The B3LYP level was considered insufficient, and the $\rho(r)$ function obtained at MP2 level of theory was chosen for further discussion.

TABLE 4: Comparison of Integral Properties of Sulfur Atomic Basins for Conformers 1, 1A, 1B, 1C and 1D

conformer	atom label	$N(\Omega)$, e	$E(\Omega)$, a.u	ΔE (Ω), kcal/mol	$\Delta N(\Omega)$, e
1B	S(1)	15.9446	−397.8159	0.00	0.000
1	S(1)	15.9954	−397.8373	−13.43	0.051
1C	S(1)	15.8920	−397.8225	−4.14	−0.053
1C	S(2)	16.0030	−397.8443	−17.82	0.058
1A	S(1)	15.8986	−397.8203	−2.76	−0.046
1D	S(1)	15.9778	−397.8486	−20.52	0.033

TABLE 5: Comparison of Integral Properties of Nitrogen Atomic Basins for Conformers 1, 1A, 1B, 1C and 1D

conformer	atom label	$N(\Omega)$	$E(\Omega)$	ΔE (Ω), kcal/mol	$\Delta N(\Omega)$
1B	N(1)	7.6744	−54.9612	0.00	0.000
1	N(1)	7.6430	−54.9360	15.81	−0.031
1C	N(1)	7.6428	−54.9002	38.28	−0.032
1A	N(1)	7.6539	−54.9105	31.81	−0.021
1D	N(1)	7.6526	−54.9068	34.14	−0.022

As the reference point for estimation of stereoelectronic interaction energies it is reasonable to choose not the energy minimum but the conformer in which at least *lp*-N−C−S and *lp*-N−N−C interactions are absent, i.e., the conformer **1B** (see Figure 3 and Table S5). The summary of energies and electronic populations for atomic basins of all conformers compared to those of conformer **1B** are presented in Tables 4–7.

Discussion

On the basis of previously published results[13], as well as the data obtained, we can assume that in terms of AIM theory the *lp*-N−Y−Z stereoelectronic interaction causes loss of electronic population by the Y atom and gain of it by the Z one. The atom's energy in such systems decreases with the increase of electronic populations, if no other interactions are involved[13]. The energy of such interactions can be evaluated by NBO analysis (see Tables S4−S8). The latter shows that the *lp*-N−C−S interactions (10−12 kcal/mol) are stronger than any other ones in the system studied and that the energy of *lp*-N−C−H interactions can vary in a wide range (2−6.5 kcal/mol), almost attaining the energy of *lp*-N−N−C ones (7 kcal/mol).

The stereoelectronic interactions explain the decrease of nitrogen atoms electronic population in conformer **1B** as a result of the *lp*-N−N−C interaction. At the same time, in the conformers **1A**, **1C** and **1D** where the *lp*-N−N−C stereoelectronic interactions according to both geometrical properties and NBO data (Table S4−S8) are not present, the nitrogen atoms also lose charge in comparison to conformer **1**. This fact allows us to assume that the system is also affected by repulsive interaction between adjacent nitrogen's lone pairs, which should

TABLE 6: Comparison of Integral Properties of Carbon Atomic Basins for Conformers 1, 1A, 1B, 1C and 1D

conformer	atom label	C−H bond length, Å	$N(\Omega)$	$E(\Omega)$	ΔE (Ω), kcal/mol	$\Delta N(\Omega)$
1B	C(1)	1.458	5.7702	−37.7860	0.00	0.000
1	C(1)	1.488	5.8324	−37.8250	−24.47	0.062
1	C(2)	1.440	5.7165	−37.7574	17.95	−0.054
1C	C(1)	1.474	5.8046	−37.8181	−20.14	0.034
1C	C(2)	1.461	5.7827	−37.8042	−11.42	0.013
1A	C(1)	1.464	5.7854	−37.8045	−11.61	0.015
1D	C(1)	1.464	5.7737	−37.7949	−5.58	0.003

TABLE 7: Comparison of Integral Properties of Hydrogen Atomic Basins for Conformers 1, 1A, 1B, 1C and 1D

conformer	atom label	C−H bond length, Å	$N(\Omega)$	$E(\Omega)$	ΔE (Ω), kcal/mol	$\Delta N(\Omega)$
1B	H(1E)	0.9509	−0.6075	0.00	0.000	1.089
1B	H(1A)	0.9726	−0.6147	−4.52	0.022	1.091
1	H(1A)	0.9676	−0.6168	−5.84	0.017	1.091
1	H(1E)	0.9501	−0.6084	−0.56	−0.001	1.097
1	H(2E)	0.9542	−0.6086	−0.69	0.003	1.091
1	H(2A)	0.9395	−0.6072	0.19	−0.011	1.099
1C	H(1A)	0.9722	−0.6149	−4.64	0.021	1.100
1C	H(1E)	0.9476	−0.6063	0.75	−0.003	1.091
1C	H(2A)	0.9550	−0.6125	−3.14	0.004	1.093
1C	H(2E)	0.9516	−0.6051	1.51	0.001	1.092
1A	H(1A)	0.9919	−0.6216	−8.85	0.041	1.103
1A	H(1E)	0.9444	−0.6038	2.32	−0.006	1.092
1D	H(1E)	0.9536	−0.6085	−0.63	0.003	1.090
1D	H(1A)	0.9592	−0.6158	−5.21	0.008	1.093

be strong in conformers **1A**, **1C** and **1D** (eclipse conformation of lone pairs), weak in conformer **1** (*gauche* conformation, *lp*-N−N-*lp* pseudotorsion angle is ∼50°), and completely absent in the conformer **1B** with antiperiplanar arrangement of lone pairs (Figure 3).

As the interaction of neighboring lone pairs is destabilizing, the system compensates for it by a decrease of nitrogen's electronic populations. According to the data obtained, the charge "leakage" from nitrogens to neighboring carbons leads to increase of their electronic populations and consequent decrease of atom's energy value (Tables 5 and 6). Due to the above reasons the lowest charge is observed for C(2) atom in conformer **1**, which is involved in the *lp*-N−C−S interaction and not compensated by charge leakage from the nitrogens (Table 6). It is noteworthy that the *lp*-N−N-*lp* repulsion (lp−lp) is not reflected in the NBO data (Table S4−S8). From our point of view it can be estimated only by comparison of integral properties of nitrogen atomic basins in different conformers, as the $\Delta E(\Omega)$ appears to be defined by this effect. Indeed, the N(1) atom in the conformer **1B**, in which the lp−lp repulsion is *a priori* absent, is characterized by the lowest energy among the conformers studied (Table 5). In contrast, the nitrogen atom energy in **1** (*lp*-N(1)−N(1A)-*lp* is 50.2°) is higher by 15 kcal/mol, and in conformers **1A**, **1C** and **1D** with *lp*-N(1)−N(1A)-*lp* angles of 0°, independently from the steric environment and different stereoelectronic interactions, the energy value is higher by 32−38 kcal/mol with respect to the conformer **1B**.

Although according to NBO data the *lp*-N−C−H interactions are weaker than *lp*-N−C−S ones (Tables S4−S8), they significantly affect the $E(\Omega)$ and $N(\Omega)$ of hydrogens. The $N(\Omega)$ for hydrogens linearly correlated with C−H bond length with CC value equal to 97.4%.[41] This supports the conventional explanation of steroelectronic interactions in terms of charge transfer; i.e., the increase of $X^+{=}C\cdots H^-$ resonance structure contribution leads to an increase of C−H bond length and hydrogen's charge.

The NBO analysis is unable to predict these interactions quantitatively: the changes in $E(\Omega)$ and $N(\Omega)$ of hydrogens are more sensitive to the *lp*-N−C−S pseudotorsion angle value than NBO mixing energies. The values of ∼2 kcal/mol for the latter are observed even for almost unfavorable *lp*-N−C−H interactions like *lp*-N(1)−C(1)−H(1E) in conformer **1B** (Table S5), for which the $E(\Omega)$ and $N(\Omega)$ values remain almost the same. On the other hand, strong *lp*-N−C−H interactions are reflected by both NBO and AIM data resulting in NBO mixing energy exceeding 4 kcal/mol and a significant (>0.01 e) increase of hydrogen's electronic population.

The most pronounced trends in energy and electronic populations were observed for carbon atoms. The examination of the corresponding parameters (Table 6) shows that stereoelectronic interactions with sulfur lone pairs do not affect carbon's electronic populations significantly, which agrees with results of NBO analysis. The differences in electronic populations can be explained explicitly by stereoelectronic interactions with nitrogen's lone pairs, and the **1B**-C(1) electronic population appears to be very close to the mean of **1**-C(1) and **1**-C(2) electronic populations, although it should be affected by *lp*-S−C−N stereoelectronic interaction predicted by NBO.

On the other hand, the *lp*-N−C−S, *lp*-N−C−H and *lp*-N−N−C stereoelectronic interaction should increase the contribution of the $N^+{=}C\cdots S^-$, $N^+{=}C\cdots H^-$ and $N^+{=}N\cdots C^-$ resonance structures, which in turn will be reflected in the variation of corresponding bond lengths. The charge transfer from N to C caused by nitrogen lone pair repulsion also should affect the C−N bond length. Thus, the length of the C−N bond can be chosen as a quantitative measure of the sum of all nitrogen−carbon stereoelectronic interactions in the structure studied. The simple linear fit of carbon's $N(\Omega)$ to C−N bond length has shown that these values correlate linearly with CC > 98%.[42] Thus, the differences in electronic populations of carbons in the conformers studied are caused solely by nitrogen−carbon interaction, and the role of interactions of sulfur lone pairs should be considered insignificant. The correlation is method-dependent but stays linear: three carbons, for which $N(\Omega)$ was calculated at B3LYP level, followed another linear correlation. It should be noted that in the case of NBO data the same correlation with C−N bond lengths failed.

As the sulfur atoms are involved only in *lp*-N−C−S stereoelectronic interactions, the changes in their $E(\Omega)$ and $N(\Omega)$ values can be predicted by NBO. The *lp*-N−C−S interaction with NBO mixing energy of ∼10 kcal/mol leads to an increase of sulfur's $N(\Omega)$ and a corresponding decrease of $E(\Omega)$. It is important to indicate that the change of $E(\Omega)$ has a value of 10−20 kcal/mol, which is comparable with the NBO mixing energy. At the same time, significant differences in $N(\Omega)$ for sulfur atoms, which are not involved in *lp*-N−C−S interactions, namely, S(1) in conformers **1A**, **1B** and **1C** (see Table 4), cannot be predicted by analysis of stereoelectronic interactions. Appartently, the charge leakage from the S(1) in conformers **1A** and **1C** has the same nature as for nitrogen atoms, i.e., the "through space" interaction of sulfur and nitrogen lp's.

Conclusion

The results of combined experimental and theoretical investigation of **1** have unambiguously demonstrated that the accuracy of electron density function derived from X-ray diffraction analysis is high enough to estimate the influence of stereoelectronic interactions on the atomic energy, although in **1** the difference in energies between carbon atoms involved and not involved in N−C−S stereoelectronic interaction in crystal could not be chosen as the only parameter for the estimation of stereoelectronic interactions. However, in many molecules where two independent atoms have similar chemical environments differing only by involvement in stereoelectronic interactions, the comparison of the experimentally obtained atomic energies of these atoms should result in direct estimation of the influence of this stereoelectronic interaction on the atomic energy. Furthermore, such high-resolution X-ray diffraction investigations can be used for analysis of stereoelectronic interactions for crystals with two or more independent molecules as well as conformation polymorphs.

It was shown that the electronic populations and energies of atoms in **1** estimated within quantum theory of atoms in molecules for N−C−S system follows the same trends as it was previously described for N−C−N and O−C−O ones. At the same time we can conclude that NBO analysis is insufficient for describing the stereoelectronic interactions in this system, especially for the sulfur atoms. The energy of the system can also be affected by *lp*-N–N-*lp* interactions, which are not reflected in the NBO data. Taking into account that at least the electronic populations of carbons in the system studied are linearly correlated with the C−N bond length at different calculation levels, we can suggest that even the geometric data obtained from X-ray diffraction experiments can be used for quantitative estimation of the fine electronic properties of a molecule.

Acknowledgment. This article is dedicated to the 60th birthday of Prof. V. G. Tsirelson, an outstanding scientist in the field of charge density analysis. This study was financially supported by the Russian Foundation for Basic Research (Project 06-03-32557), the Foundation of the President of the Russian Federation (Federal Program for the Support of Young Doctors, Grant MD-172.2008.3) and the Russian Science Support Foundation.

Supporting Information Available: Tables of crystallographic bond lengths and angles, cif file, data of multipole refinement, summary of intermolecular critical points (3, −1) in crystal, maps of residual electronic density and lists of symmetrically independent $n \rightarrow \sigma^*$ NBO interactions in all conformers studied. This information is available free of charge via the Internet at http://pubs.acs.org.

References and Notes

(1) Edward, J. T. *J. Chem. Ind.* **1955**, 1102.
(2) Eliel, E. L. *Angew. Chern. Int. Ed. Engl.* **1972**, *11*, 739.
(3) Kirby, J. *The Anomeric Effect and Related Stereoelectronic Effects of Oxygen*; Springer-Verlag: Berlin, 1983.
(4) Deslongchamps, P. *Stereoelectronic Effects in Organic Chemistry*; Wiley: New York, 1983.
(5) Grein, F.; Deslongchamps, P. *Can. J. Chem.* **1992**, *70*, 604.
(6) Grein, F.; Deslongchamps, P. *Can. J. Chem.* **1992**, *70*, 1562.
(7) Brunck, T. K.; Weinhold, F. *J. Am. Chem. Soc.* **1978**, *101*, 1700.
(8) Salzner, U.; Schleyer, P. v. R. *J. Am. Chem. Soc.* **1993**, *115*, 10231.
(9) Salzner, U.; Schleyer, P. v. R. *J. Org. Chem.* **1994**, *59*, 2138.
(10) Radom, L.; Hehre, W. J.; Pople, J. A. *J. Am. Chem. Soc.* **1972**, *94*, 2371.
(11) Bader, R. F. W. *Atoms In molecules. A Quantum Theory*; Clarendron Press: Oxford, U.K., 1990.
(12) Vila, A.; Mosquera, R. A. *J. Comput. Chem.* **2007**, *28*, 1516.
(13) Eskandari, K.; Vila, A.; Mosquera, R. A. *J. Phys. Chem. A* **2007**, *111*, 8491.
(14) Koritsanszky, T. S.; Coppens, P. *Chem. Rev.* **2001**, *101*, 1583.
(15) Tsirelson, V. G.; Ozerov, R. P. *Electron density and Bonding in Crystals: Principles, Theory and X-Ray Diffraction experiments in Solid State Physics And Chemistry*; IOP Publishing Ltd.: 1996.
(16) (a) Tsirelson, V. G. *Acta Crystallogr.* **2002**, *B58*, 632. (b) Zhurova, E. A.; Tsirelson, V. G.; Stash, A. I.; Yakovlev, M. V.; Pinkerton, A. A. *J. Chem. Phys.* **2004**, *108*, 20173.
(17) (a) Espinosa, E.; Molins, E.; Lecomte, C. *Chem. Phys. Lett.* **1998**, *285*, 170. (b) Espinosa, E.; Alkorta, I.; Rozas, I.; Elguero, J.; Molins, E. *Chem. Phys. Lett.* **2001**, *336*, 457.
(18) (a) Lyssenko, K. A.; Nelyubina, Yu. V.; Kostyanovsky, R. G.; Antipin, M. Yu. *ChemPhysChem* **2006**, *7*, 2453. (b) Lyssenko, K. A.; Korlyukov, A. A.; Golovanov, D. G.; Ketkov, S. Yu.; Antipin, M. Yu. *J. Phys. Chem. A* **2006**, *110*, 6545. (c) Lyssenko, K. A.; Korlyukov, A. A.; Antipin, M. Yu. *Mendeleev Commun.* **2005**, 90. (d) Glukhov, I. V.; Lyssenko, K. A.; Korlyukov, A. A.; Antipin, M. Yu. *Faraday Discuss.* **2007**, *135*, 203.
(19) Sheldrick, G. M. *SHELXTL-Plus Reference Manual*, version 5.0; Siemens Analytical X-ray Instruments Inc.: Madison, WI, 1996.
(20) Hansen, N. K.; Coppens, P. *Acta Crystallogr., Sect. A* **1978**, *34*, 909.
(21) Koritsansky, T. S.; Howard, S. T.; Richter, T.; Macchi, P.; Volkov, A.; Gatti, C.; Mallinson, P. R.; Farrugia, L. J.; Su, Z.; Hansen, N. K. *XD - A Computer program package for multipole refinement and Topological Analysis of charge densities from diffraction data*, 2003.
(22) Su, Z.; Hansen, N. K. *Acta Crystallogr., Sect. A* **1998**, *54*, 646.
(23) Worsham Junior, J. E.; Busing, W. R. *Acta Crystallogr., Sect. B* **1969**, *25*, 572.
(24) Stash, A.; Tsirelson, V. WinXPRO, A program for Calculation of the Crystal and Molecular properties Using the Model Electron Density, 2001. *Acta Crystallogr.* **2002**, *35*, 371.
(25) Kirzhnits, D. A. *Sov. Phys. JETP* **1957**, *5*, 64.
(26) Zhurova, E. A.; Tsirelson, V. G.; Stash, A. I.; Yakovlev, M. V.; Pinkerton, A. A. *J. Phys. Chem. B* **2004**, *108*, 20173.
(27) Tsirelson, V. G. *Acta Crystallogr.* **2002**, *B58*, 632.
(28) Frisch, M. J.; Trucks, G. W.; Schlegel, H. B.; Scuseria, G. E.; Robb, M. A.; Cheeseman, J. R.; Zakrzewski, V. G.; Montgomery, J. A.; Stratmann, R. E.; Burant, J. C.; Dapprich, S.; Millam, J. M.; Daniels, A. D.; Kudin, K. N.; Strain, M. C.; Farkas O.; Tomasi, J.; Barone, V.; Cossi, M.; Cammi, R.; Mennucci, B.; Pomelli, C.; Adamo, C.; Clifford, S.; Ochterski, J.; Petersson, G. A.; Ayala, P. Y.; Cui, Q.; Morokuma, K.; Malick, D. K.; Rabuck, A. D.; Raghavachari, K.; Foresman, J. B.; Cioslowski, J.; Ortiz, J. V.; Stefanov, B. B.; Liu, G.; Liashenko, A.; Piskorz, P.; Komaromi, I.; Gomperts, R.; Martin, R. L.; Fox, D. J.; Keith, T.; Al-Laham, M. A.; Peng, C. Y.; Nanayakkara, A.; Gonzalez, C.; Challacombe, M.; Gill, P. M. W.; Johnson, B. G.; Chen, W.; Wong, M. W.; Andres, J. L.; Head-Gordon, M.; Replogle, E. S.; Pople, J. A. *Gaussian 98*, revision A.7; Gaussian, Inc.: Pittsburgh, PA, 1998.
(29) Allinger, N. L.; Yuh, Y. H.; Lii, J.-H. *J. Am. Chem. Soc.* **1989**, *111*, 8551.
(30) Popelier, P. L. A. *Comput. Phys. Commun.* **1996**, *93*, 212.
(31) (a) Popelier, P. L. A. *Theor. Chim. Acta* **1994**, *87*, 465. (b) Popelier, P. L. A. *Mol. Phys.* **1996**, *87*, 1169.
(32) Rowland, R. S.; Taylor, R. *J. Phys. Chem.* **1996**, *100*, 7384.
(33) Gillespie, R. J., Hargittai, I. *The VSEPR Model of Molecular Geometry*; Allyn and Bacon: London, 1991.
(34) Tsirelson, V.; Stash, A. *Chem. Phys. Lett.* **2002**, *351*, 142.
(35) (a) Lyssenko, K. A.; Grintselev-Knyazev, G. V.; Antipin, M. Yu. *Mendeleev Commun.* **2002**, 128. (b) Lyssenko, K. A.; Antipin, M. Yu.; Gurskii, M. E.; Bubnov, Yu. N.; Karionova, A. L.; Boese, R. *Chem. Phys. Lett.* **2004**, *384*, 40.
(36) Savin, A.; Silvi, B.; Colonna, F. *Can. J. Chem.* **1996**, *74*, 1088.
(37) Ouvrard, C.; Mitchell, J. B. O. *Acta Crystallogr.* **2003**, *B59*, 676.
(38) (a) Lyssenko, K. A.; Antipin, M. Yu.; Gurskii, M. E.; Bubnov, Yu. N.; Karionova, A. L.; Boese, R. *Chem. Phys. Lett.* **2004**, *384*, 40. (b) Zhurova, E. A.; Tsirelson, V. G.; Stach, A. I.; Pinkerton, A. A. *J. Am. Chem. Soc.* **2002**, *124*, 4574. (c) Lyssenko, K. A.; Aldoshin, S. M.; Antipin, M. Yu. *Mendeleev Commun.* **2004**, 98.
(39) Matta, C. F.; Arabi, A. A.; Keith, T. A. J. *Phys. Chem. A* **2007**, *111*, 8864.
(40) Graňa, A. M.; Mosquera, R. A. *J. Chem. Phys.* **1999**, *110*, 6606.
(41) The correlation of hydrogen's electronic population with C−H length was obtained by least-squares refinement and led to linear dependence with equation $N = -2.1133 + 2.8075X$, where N is $N(\Omega)$, in au, and X is the C−H length, in Å, standard deviation = 0.0027 and correlation coefficient = 97.4%.
(42) The correlation equation is $N = 2.309 + 2.37183*X$, where X is the C−N bond length and N is the electronic population of carbon. The data (Table S12) fit the equation with a correlation coefficient of 98.6% and a standard deviation of 0.00638.

JP800384K